Sharp Toroidal Resonances in Planar Terahertz Metasurfaces

Gupta, Manoj; Savinov, Vassili; Xu, Ningning; Cong, Longqing; Dayal, Govind; Wang, Shuang; Zhang, Weili; Zheludev, Nikolay I.; Singh, Ranjan

2016

Gupta, M., Savinov, V., Xu, N., Cong, L., Dayal, G., Wang, S., et al. (2016). Sharp Toroidal Resonances in Planar Terahertz Metasurfaces. Advanced Materials, 28(37), 8206-8211.

https://hdl.handle.net/10356/83782

https://doi.org/10.1002/adma.201601611

Sharp toroidal resonances in planar terahertz metasurfaces

By *Manoj Gupta, Vassili Savinov, Ningning Xu, Longqing Cong, Govind Dayal, Shuang Wang, Weili Zhang, Nikolay I. Zheludev*, and *Ranjan Singh*[*]

M. Gupta, L. Cong, G. Dayal, Prof. N.I. Zheludev, Prof. R. Singh
Division of Physics and Applied Physics, School of Physical and Mathematical Sciences, Nanyang Technological University, Singapore 637371, Singapore
Centre for Disruptive Photonic Technologies, School of Physical and Mathematical Sciences, Nanyang Technological University, Singapore 637371, Singapore
E-mail: ranjans@ntu.edu.sg

V. Savinov, Prof. N.I. Zheludev
Optoelectronics Research Centre
University of Southampton, UK
E-mail: niz@orc.soton.ac.uk

N. Xu, Prof. W. Zhang
School of Electrical and Computer Engineering
Oklahoma State University
Stillwater, OK 74078
E-mail: weili.zhang@okstate.edu

S. Wang
Department of Electronic Engineering
Tianjin University of Technology and Education
Tianjin 300222, China
E-mail: homehv236@gmail.com

Keywords: Toroidal, metasurface, terahertz, magnetic coupling

Metamaterials are composite arrays of artificially structured materials, where the dimension of the unit cell of the array is sufficiently smaller than the wavelength of the incident radiation. These artificially designed subwavelength structures have attracted tremendous attention in the photonics community over the last decade. By tailoring the geometry of the unit cells, many exotic phenomena could be realized, which have immense application potential such as super lensing,[1] negative index media,[2] plasmonic biosensors, metamaterial absorbers,[3] and reconfigurable metadevices.[4] The desired electromagnetic response in metamaterials is

achieved by properly designing its meta-molecules in such a way that resonantly excited unit cells can be represented in terms of few key multipole excitations, such as electric and magnetic dipoles. The overall effective metamaterial response can then be determined through a homogenization procedure, in close similarity to electromagnetic response in natural media. Recently, the attention of metamaterial community has been attracted by the virtually unknown third family of electromagnetic multipoles, the toroidal multipoles, which along with the familiar electric and magnetic multipoles is necessary for the complete multipole representation of an arbitrary radiating source. The toroidal dipole can be viewed as a circular head-to-tail arrangement of magnetic dipoles, all squeezed into a single point.[5] It was first reported by Zel'dovich in the context of nuclear and particle physics.[6] Toroidal dipole is not a part of standard multipole expansion despite corresponding to a unique current density. The interaction energy of toroidal dipole depends on the time derivatives of electromagnetic fields, rather than on field themselves. Far field radiation pattern of toroidal dipole is indistinguishable from that of the electric dipole.[7] So far, toroidal moments have been found in molecule structures,[8] and ferroelectric systems.[9] Recently, toroidal dipolar response was demonstrated in metamaterials.[10-14] It has been shown that artificial media with strong toroidal dipole response exhibits many unique electromagnetic phenomena such as resonant transparency,[15] unconventional optical activity,[16-19] and could even give rise to negative index of refraction.[20] Usually the response due to toroidal dipole (currents flowing on the surface of a torus along its meridians) is masked by other electric and magnetic multipoles, which are simultaneously excited during the interaction of resonator with electromagnetic wave. This makes the detection of toroidal excitation quite challenging.[21] However, the toroidal dipole response can be enhanced through meta-molecule design. One should aim to supress the excitation of electric and magnetic dipoles as well as electric and magnetic quadrupoles. Simultaneously one should aim to confine the magnetic field inside the metamolecules into tight oscillating loops, this arrangement corresponding directly to the

toroidal dipole excitation. Many three-dimensional (3D) structures have been suggested in experimental and simulation papers which manifest strong toroidal response.[22-25] However, as the size of metamolecules approaches micro and nano-scale, due to limitations of fabrication, the realization of a true 3D structure becomes quite challenging**.** In this paper we would show a strong toroidal dipole that could be achieved in a 2D metamaterial which is fabricated in a single step lithography cycle.

Compared with 3D metamaterials, the 2D metamaterials offer relatively poor confinement of circulating magnetic field, nevertheless, by careful choice of metamaterial geometry, one can supress all unwanted multipoles to reveal the toroidal dipole contribution. In this paper we focus our study on toroidal dipolar response in the terahertz region in a two-dimensional (2D) metamaterial structure as shown in **Figure 1**a. Our metamaterial design is based on two joint metallic loops with two capacitive gaps in each loop. By controlling the position of the gaps and the polarization of the incident field it is possible, in this metamaterial, to excite a resonant mode in which the currents in the two loops of each metamolecule oscillate in opposite directions. Due to the position of the gaps, this mode results in a supressed electric and enhanced toroidal dipole response. One can contrast this with the well-known ELC metamaterial, in which the counter-propagating currents in the two loops of the metamolecule result in a strong electric dipole response, which masks all other multipole excitations. [26]

For the purpose of analysis, it will be assumed throughout this paper that the metamaterial is excited by the plane-wave radiation at normal incidence. It follows, that all the metamolecules will be oscillating in-phase with each other. It has previously been shown that in such conditions one can represent the plane-wave scattering of the whole metamaterial using in-plane projections of multipolar representation of the scattering by a single metamolecule.[27] Assuming that the metamaterial array lies in the XY-plane, we can limit our attention to the projection of the toroidal dipole in this plane, which is given by $\mathbf{T}_{\parallel} = \mathrm{T}_x\hat{\mathbf{x}} + \mathrm{T}_y\hat{\mathbf{y}}$, where $\hat{\mathbf{x}}, \hat{\mathbf{y}}$

are the unit vectors along the X, and Y direction. The subscript $(\ldots)_{\parallel}$ denotes the projection of vector into the metamaterial plane. We have dropped the z-component of the dipole because it has been shown that in case of scattering by an array of dipoles lying in the XY-plane, the z-components of the individual dipole scattering does not contribute to the net radiation from the array. Far field component of electric field ($\mathbf{E_{s-t}}$) scattered by an array of identical toroidal dipoles are given by the equation:

$$\vec{\mathbf{E}}_{\mathbf{s-t}} = -\frac{\mu_o c^2 k^2}{2\Delta^2}\vec{\mathbf{T}}_{\parallel}\exp(-ikR) \qquad (1)$$

If we consider first eight dynamic multipoles, then electric field (E_s) emitted by the array with induced oscillations of charge-current density can be given by the equation[27] approximately as

$$\vec{\mathbf{E}}_{\mathbf{s}} = \frac{\mu_o c^2}{2\Delta^2}\left[-ik\vec{\mathbf{p}}_{\parallel} + ik\hat{\mathbf{R}}\times\left(\vec{\mathbf{m}}_{\parallel} - \frac{k^2}{10}\vec{\mathbf{m}}^{(1)}_{\parallel}\right) - k^2\left(\vec{\mathbf{T}}_{\parallel} + \frac{k^2}{10}\vec{\mathbf{T}}^{(1)}_{\parallel}\right) + k^2\left(\vec{\mathbf{Q}}^{(e)}.\hat{\mathbf{R}}\right)_{\parallel}\right.$$
$$-\frac{k^2}{2}\hat{\mathbf{R}}\times\left(\vec{\mathbf{Q}}^{(m)}.\hat{\mathbf{R}}\right)_{\parallel} - \frac{ik^3}{3}\left(\vec{\mathbf{Q}}^{(T)}.\hat{\mathbf{R}}\right)_{\parallel} + ik^3\left(\left(\vec{\mathbf{O}}^{(e)}.\hat{\mathbf{R}}\right).\hat{\mathbf{R}}\right)_{\parallel}$$
$$\left.-\frac{ik^3}{180}\left(\hat{\mathbf{R}}\times\left(\left(\vec{\mathbf{O}}^{(m)}.\hat{\mathbf{R}}\right).\hat{\mathbf{R}}\right)_{\parallel}\right)\right].\exp(-ikR) \qquad (2)$$

Other higher order terms can be neglected, due to their extremely weak influence on the scattered intensity. Here c is the speed of light, k is the wave number, μ_0 is the magnetic permeability, Δ^2 denotes the area of the unit cell, R is the perpendicular distance of observer from the planar array, and $\hat{\mathbf{R}}$ is the unit vector perpendicular to plane of array (pointing towards the observer). Above Equation (2) contains ten terms corresponding to the electric (**p**), toroidal (**T**) and magnetic (**m**) dipoles, electric ($\mathbf{Q^{(e)}}$), magnetic ($\mathbf{Q^{(m)}}$) and toroidal ($\mathbf{Q^{(T)}}$) quadrupoles, electric ($\mathbf{O^{(e)}}$) and magnetic ($\mathbf{O^{(m)}}$) octupoles, and the so-called mean square radii of toroidal ($\mathbf{T}^{(1)}$) and magnetic ($\mathbf{m}^{(1)}$) dipoles, which are the lowest-order corrections retained

to account for the finite size of the metamolecules.[28] The radiation transmitted by the two dimensional array, can be found by adding up the incident and scattered radiation by the array.

$$\vec{\mathbf{E}}_{\text{transmitted}} = [\vec{\mathbf{E}}_s]_{\hat{\mathbf{R}}=\hat{\mathbf{k}}} + \vec{\mathbf{E}}_{\text{incident}} \quad (3)$$

Where '$\hat{\mathbf{k}}$' unit vector points in the direction (+ Z) of propagation of incident radiation.

In this work, we have demonstrated the variation in toroidal dipolar response, by symmetrically moving the pair of capacitive gaps toward central branch of the SRR in the unit cell structure (as shown in Figure 1b), and the effect of toroidal component on the overall scattered intensity of the transmitted light.

We analyze the electromagnetic response of an infinite two dimensional array of toroidal metamolecules. Figure 1b shows the schematic diagram of unit cell of toroidal metamaterial with its design parameters. The unit cell of metamaterial consists of two double split square shaped SRRs, merged to form single enlarged double ring SRR with four split gaps. Figure 1c shows the microscopic image of the array of SRRs fabricated from 200 nm thick aluminum (Al) on 500 μm thick high resistivity p-type silicon substrate. The outer dimension of individual resonator is 120 μm × 60 μm and the periodicity of the array is 150 μm × 75 μm. Line width of arm of the resonator is 6 μm and the split-gap size is 3 μm. The electromagnetic field excites the sample at normal incidence, having its electric field component perpendicular to the gaps in the metamolecules. Initially both the gap pair on the left and right side of central vertical arm are at same distance 30 μm (d = 0 position) from the side branch as shown in the zoomed unit cell inset of Figure 1b. Simulations and experiments have been performed by moving the gap pairs symmetrically by distance d towards the central branch. In simulations, the material parameters of metals were described using the Drude model, where frequency dependent permittivity is given by given by $\varepsilon(\omega) = \varepsilon_\infty - \left[\omega_p^2 / \omega(\omega + i\Gamma) \right]$, with the plasma

frequency ω_p (22.43×10^{15} rad/sec for Al) and damping rate Γ (124.34×10^{12} rad/sec).[29] Toroidal resonance can be excited by the incident field (E_x) polarized perpendicular to the gaps.

Figure 2a-d shows the simulated and measured transmittance of metamaterial samples with different shifts of the gap (towards the central lines of the metamolecules). As *d* changes, the asymmetric toroidal resonance first disappears (d~5 μm) and then again reappears for higher asymmetry. The line width of toroidal resonance first decreases then increases as a function of *d*. The *Q* factor of narrow resonance has been determined by taking into account the highest peak and lowest dip of the transmittance curve. In this paper, the *Q*-factor is defined as the ratio of resonance frequency to the full width at half maximum (FWHM). There is a good agreement between the measured and simulated transmission spectra of the metamaterial, some variations between simulated and measured results could be due to the imperfections arising from the fabrication process.

We will now analyse the role of toroidal multipoles in determining the electromagnetic response of the metamaterial. As we move to higher order toroidal multipoles, the strength of the toroidal response weakens by two orders of magnitude. Only the toroidal dipole and toroidal quadrupole excitation provide a significant contribution to the metamaterial response. So, to simplify the analysis, all higher toroidal multipoles can therefore be ignored.

Figure 3a shows the transmittance spectra with and without toroidal multipole for the sample with gap shift of 3 μm. The transmittance value for both curves at different frequencies has been computed using Equation (1, 2, and 3). The effect of toroidal dipole excitation is to increase the transmission at frequencies below 0.4 THz, and to reduce the transmission above 0.4 THz.

Figure 3b shows the *x*-component of the toroidal dipole (T_x) excitation for metamaterials with different gap shifts *d* (metamaterial design only supports toroidal dipole along X-axis). The

relationship between the strength of toroidal excitation and the position of the gap is non-trivial: as d is increased from d=0 μm to d=3μm, the toroidal dipole excitation is supressed, whilst further increase to d=5μm and d=7 μm results in the enhancement of toroidal dipole moment. We further highlight the relationship between T_x and d by plotting the resonant strength of toroidal dipole excitation as a function of gap position in **Figure 4**. This non-trivial relationship reveals the influence of the substrate on metamaterial response. In our case the substrate is high-resistivity p-type silicon with thickness 0.5mm, which, at radiation frequency 0.4THz, corresponds to slightly above 2 wavelengths (using refractive index 3.4) .[30] As a result, the response of the metamaterial is augmented by the Fabry-Perot type cavity resonance in the substrate. This feature is deliberate, in fact it is impossible to create dominant toroidal dipole response using only planar currents. Two co-planar loops with counter-propagating currents will correspond to a mixture of magnetic quadrupole and toroidal dipole, however the displacement currents engaged in the substrate of the metamaterial act as an extra magnetic dipole. Together with the magnetic dipoles due to currents in the metallic loops, one can thus create conditions in which the toroidal dipole excitation will be dominant (head-to-tail arrangement of magnetic dipoles). Since the standing-wave mode in the dielectric slab with metamaterial on one of its faces cannot be described analytically, we have to optimize the toroidal dipole response numerically, which is accomplished by choosing an optimal gap position d (see Figure 3b and Figure 4).

The strong enhancement of toroidal dipole at the correct gap position can be illustrated by considering the current density and magnetic field induced in the metamaterials at their respective resonant frequencies, as is shown in **Figure 5**. At d=0 μm and d=3 μm, where T_x is weak, the current in the central metallic strip of the metamolecule is greater than at the edge-strips. This imbalance leads to strong electric dipole and weak toroidal dipole. At d=7 μm, where T_x is strong, the current in the three strips is roughly equal in magnitude, which results

in the enhanced toroidal dipole and weak electric dipole. Beyond *d* equal to 7 μm, again there is a large mismatch between the induced currents in side and central branch of the resonating structure (not shown here), which results in reduced toroidal dipole response.

Before concluding we would like to point out that the response of our metamaterial can be understood in terms of the well-known Fano resonance. [31] As one can see from Figure 2, the resonant response of our metamaterial is associated with an asymmetric transmission window, a hall-mark of Fano resonance, which, in our case, arises as a result of coupling between the 'bright mode' electric dipole, and the 'dark mode' toroidal dipole.

Conclusion:

We have investigated the engineered response of the sharp toroidal dipolar resonances in planar terahertz metamaterials. By tailoring the asymmetry in the structure, the linewidth, amplitude and the quality factor of the toroidal resonances is tuned. Toroidal resonances offer another route to excite low loss, high-*Q* resonances that could be exploited for metadevice applications such as ultrasensitive sensors, modulators, and lasing spasers. Our finding offers a scalable planar design for exciting toroidal modes in the terahertz regime and a similar planar design could be applied for exciting these exotic modes at higher frequencies.

Experimental Section:

Simulations: All numerical simulations were carried out in frequency domain with periodic boundary condition by using commercially available software CST Microwave Studio, and Comsol Multiphysics. Toroidal component for different frequency values have been

calculated through Matlab programs and *LiveLink™ for Matlab* feature of Comsol Multiphysics. Unit cell dimensions of the metamaterial array are specified in main text with detailed information in Figure 1b. During simulations material properties have been taken similar to experimental samples. The metadevice was excited by electromagnetic radiation having its electric field component perpendicular to the gap arm.

Sample Fabrication: Metamaterial samples were fabricated by photolithography. Positive photoresist was coated on the polished side of silicon wafer (0.50 mm thick, high resistivity p-type silicon) followed by patterning with the proper mask. With the aid of thermal evaporator 200 nm thick aluminum film was deposited on the patterned photoresist. Aluminum deposited wafers were soaked in acetone for lift-off to get the desired metallic structures.

Measurements: At normal incidence, the characterization of the fabricated samples were done at the terahertz (THz) frequencies using the terahertz time domain spectroscopy (THz-TDS) technique. The femtosecond fiber laser beam (90 fs, 60 mW at 1560 nm with 100 MHz repetition rate) was focused on a photoconductive antenna to generate and detect the terahertz signals. The normalized transmission amplitude was obtained as the ratio between the spectral fields of sample $\tilde{E}_s(\omega)$ and reference $\tilde{E}_r(\omega)$, where ω is the angular frequency. Spectral field of sample and reference was calculated by the FFT of time domain signal.

References:

[1] V. M. Shalaev, *Nat. Photonics* **2007**, *1*, 41.

[2] J. Valentine, S. Zhang, T. Zentgraf, E. Ulin-Avila, D. A. Genov, G. Bartal, X. Zhang, *Nature* **2008**, *455*, 376.

[3] N. I. Landy, S. Sajuyigbe, J. J. Mock, D. R. Smith, W. J. Padilla, *Phys. Rev. Lett.* **2008**, *100*, 207402.

[4] N. I. Zheludev, Y. S. Kivshar, *Nat. Mater.* **2012**, *11*, 917.

[5] V. M. Dubovik, V. V. Tugushev, *Phys. Rep.* **1990**, *187*, 145.

[6] I. B. Zel'dovich, *Sov. Phys. JETP* **1958**, *6*, 1184.

[7] G. N. Afanasiev, P. S. Yu, *J. Phys. A: Math. Gen.* **1995**, *28*, 4565.

[8] A. Ceulemans, L. F. Chibotaru, P. W. Fowler, *Phys. Rev. Lett.* **1998**, *80*, 1861.

[9] I. I. Naumov, L. Bellaiche, H. Fu, *Nature* **2004**, *432*, 737.

[10] T. Kaelberer, V. A. Fedotov, N. Papasimakis, D. P. Tsai, N. I. Zheludev, *Science* **2010**, *330*, 1510.

[11] Y. Fan, Z. Wei, H. Li, H. Chen, C. M. Soukoulis, *Phys. Rev. B* **2013**, *87*, 115417.

[12] Z.-G. Dong, P. Ni, J. Zhu, X. Yin, X. Zhang, *Opt. Express* **2012**, *20*, 13065.

[13] Y. Bao, X. Zhu, Z. Fang, *Sci. Rep.* **2015**, *5*, 11793.

[14] B. Ögüt, N. Talebi, R. Vogelgesang, W. Sigle, P. A. van Aken, *Nano Lett.* **2012**, *12*, 5239.

[15] H.-m. Li, S.-b. Liu, S.-y. Liu, S.-y. Wang, G.-w. Ding, H. Yang, Z.-y. Yu, H.-f. Zhang, *Appl. Phys. Lett.* **2015**, *106*, 083511.

[16] L.-Y. Guo, M.-H. Li, X.-J. Huang, H.-L. Yang, *Appl. Phys. Lett.* **2014**, *105*, 033507.

[17] N. Papasimakis, V. A. Fedotov, K. Marinov, N. I. Zheludev, *Phys. Rev. Lett.* **2009**, *103*, 093901.

[18] T. Raybould, V. Fedotov, N. Papsimakis, I. Youngs, W. T. Chen, D. P. Tsai, N. Zheludev, presented at Conf. Laser Science to Photonic App., San Jose Convention Center San Jose, CA, USA, 10-15 ((May, **2015**)).

[19] N. Papasimakis, V. A. Fedotov, V. Savinov, T. A. Raybould, N. I. Zheludev, *Nat. Mater.***2016**, *15*, 263.

[20] K. Marinov, A. D. Boardman, V. A. Fedotov, N. Zheludev, *New J. Phys.* **2007**, *9*, 324.

[21] K. Sawada, N. Nagaosa, *Phys. Rev. Lett.* **2005**, *95*, 237402.

[22] A. A. Basharin, M. Kafesaki, E. N. Economou, C. M. Soukoulis, V. A. Fedotov, V.

Savinov, N. I. Zheludev, *Phys. Rev. X* **2015**, *5*, 011036.

[23] V. A. Fedotov, A. V. Rogacheva, V. Savinov, D. P. Tsai, N. I. Zheludev, *Sci. Rep.* **2013**, *3*, 2967.

[24] Y.-W. Huang, W. T. Chen, P. C. Wu, V. Fedotov, V. Savinov, Y. Z. Ho, Y.-F. Chau, N. I. Zheludev, D. P. Tsai, *Opt. Express* **2012**, *20*, 1760.

[25] V. Savinov, V. A. Fedotov, W. T. Chen, Y. W. Huang, D. P. Tsai, D. B. Burckel, I. Brener, N. I. Zheludev, presented at Conf. Lasers Electro-Opt., San Jose Convention Center San Jose, CA, USA, 6-11 ((May, **2012**)).

[26] D. Schurig, J. J. Mock, D. R. Smith, *Appl. Phys. Lett.* **2006**, *88*, 041109.

[27] V. Savinov, V. A. Fedotov, N. I. Zheludev, *Phys. Rev. B* **2014**, *89*, 205112.

[28] E. E. Radescu, G. Vaman, *Phys. Rev. E* **2002**, *65*, 046609.

[29] M. A. Ordal, L. L. Long, R. J. Bell, S. E. Bell, R. R. Bell, R. W. Alexander, C. A. Ward, *Appl. Opt.* **1983**, *22*, 1099.

[30] D. Grischkowsky, Søren Keiding, Martin van Exter, Ch. Fattinger, *J. Opt. Soc. Am. B* **1990**, *7*, 2006

[31] B. Luk'yanchuk, N. I. Zheludev, S. A. Maier, N. J. Halas, P. Nordlander, H. Giessen, C. T. Chong, *Nat. Mater.* **2010**, *9*, 707

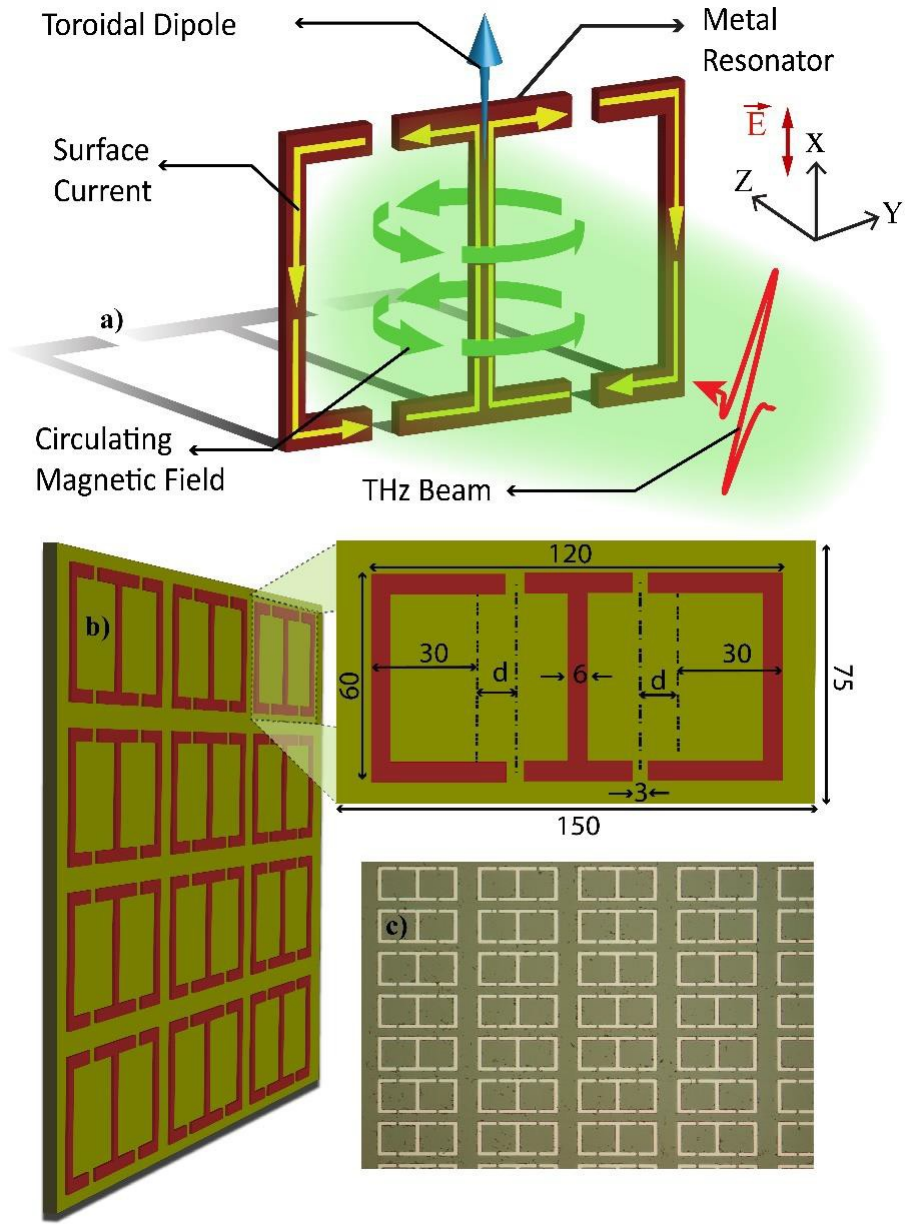

Figure 1. (a) Artistic impression of toroidal dipole generated due to circulating magnetic field produced by current carrying loops. (b) Schematic of metamaterial array and unit cell (all dimensions are in micron), gaps position changes symmetrically for different values of *d*. (c) Microscope image of fabricated sample.

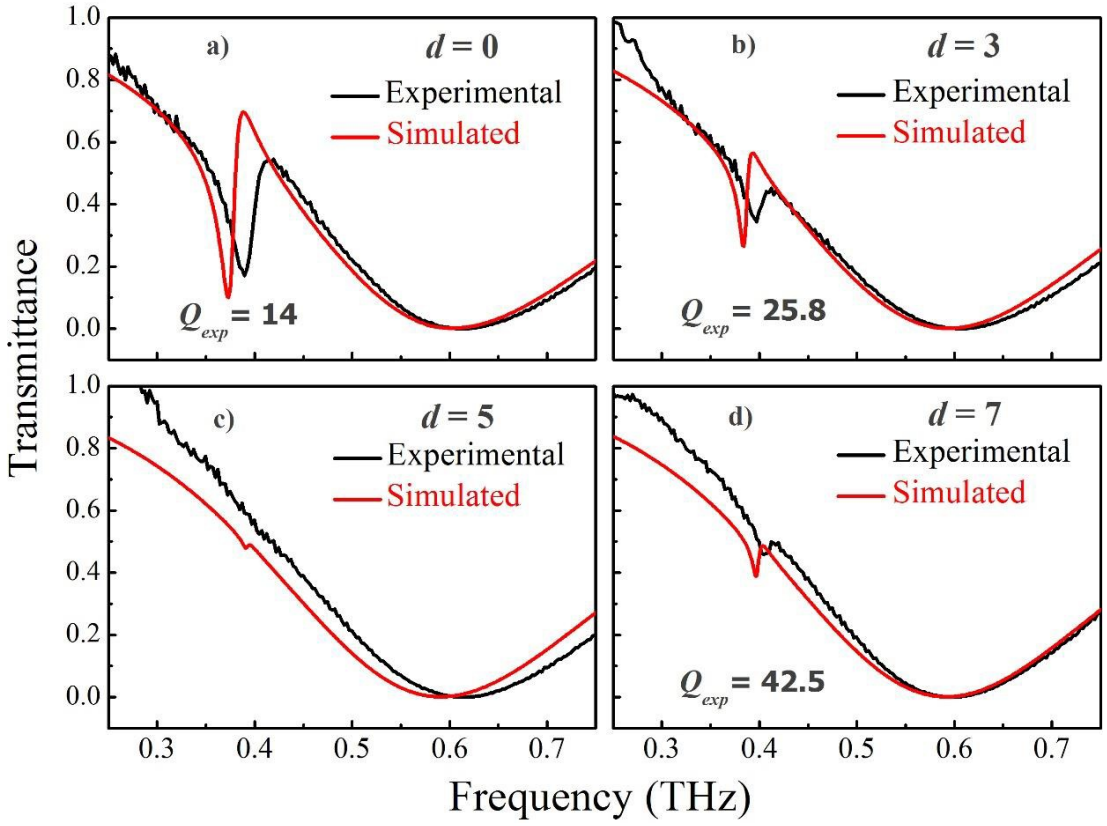

Figure 2. Experimental and simulated amplitude transmission spectra for samples having different position of gaps indicated by *d* (0, 3, 5 and 7 μm), when E field is polarized perpendicular to the gap. The quality factor of the resonances in (a, b, d) is given as a subscript.

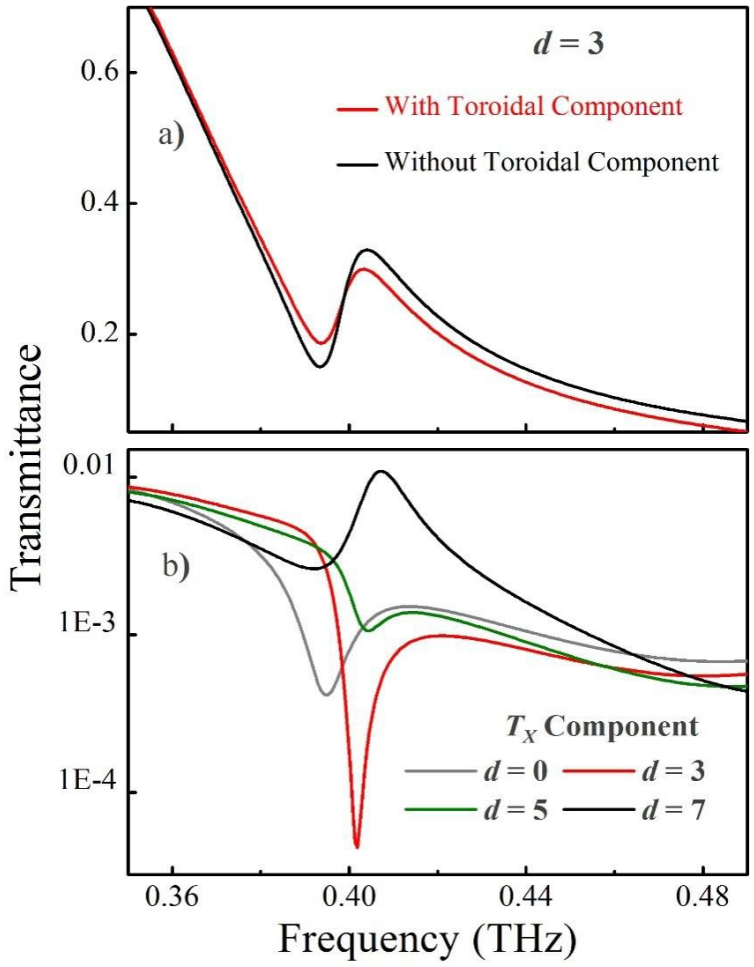

Figure 3. (a) Simulated transmitted intensity with and without toroidal component for sample having position of gaps as per d = 3 μm. (b) Variation of toroidal dipole component along X-axis for different values of d.

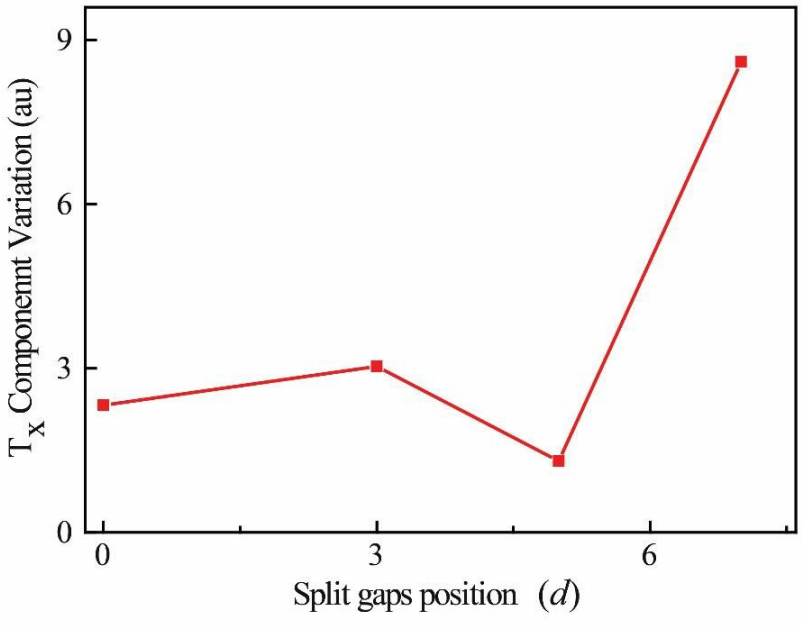

Figure 4. Magnitude of excited toroidal dipole component as a function of split gap position (*d*), at the instant of the electromagnetic resonance.

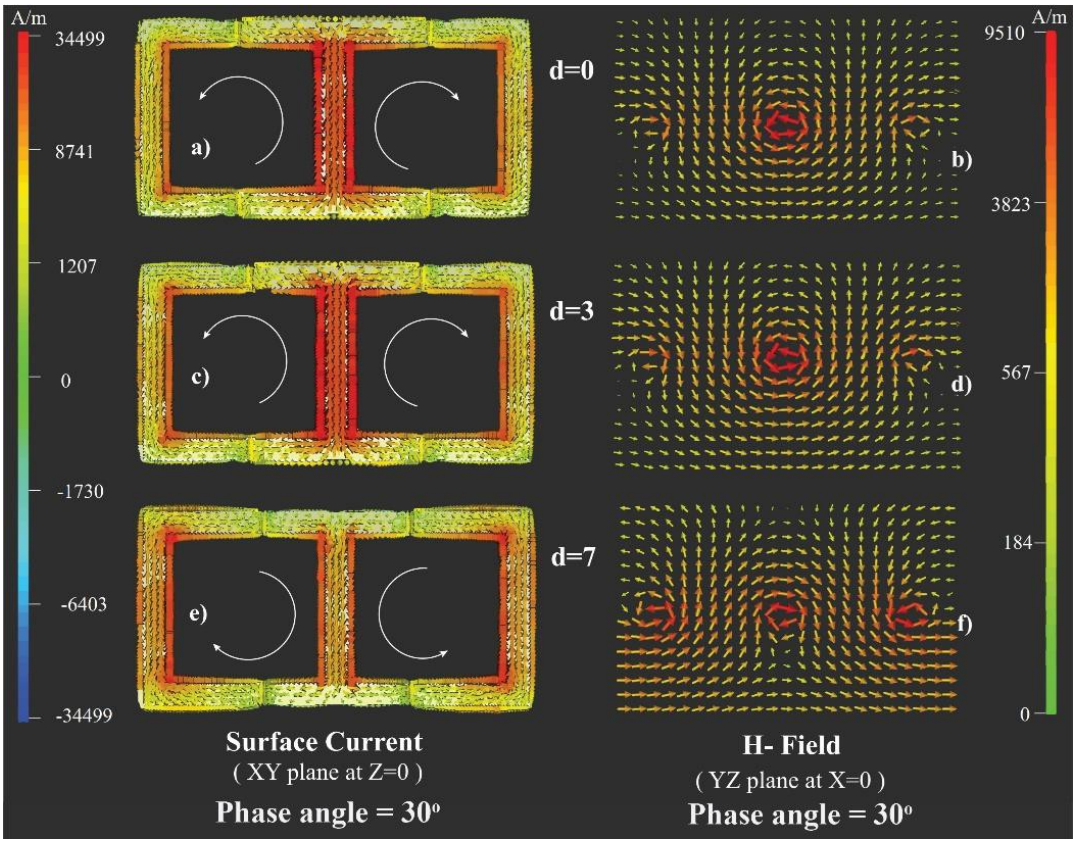

Figure 5. Simulated surface currents and H-field (on YZ plane at X=0) of resonator at narrow resonance, for different position of gaps (d = 0, 3, and 7 μm). For d = 0 and 3 μm narrow resonance occurs nearly at 0.38 THz, and for d =7 μm resonance occurs at 0.40 THz.